

A Study of the Surface Protective Layer Formed on Carbon Steel in Water-Dioxane Solution Containing 0.15 M NaCl in Presence of an azo Dye with Antimicrobial Activity

Adriana Samide¹, Bogdan Tutunaru^{1,*}, Anca Moanță^{1,*}, Cătălina Ionescu¹, Cristian Tigae¹, Ana-Cristina Vladu^{1,2}

¹ University of Craiova, Faculty of Mathematics and Natural Sciences, Department of Chemistry, Calea Bucuresti, 107i, Craiova, Romania

² Babes-Bolyai University, Faculty of Chemistry and Chemical Engineering, Str. Arany Janos no. 11, Cluj-Napoca, Romania

*E-mail: tutunarchim@yahoo.com; moantaanca@yahoo.com

Received: 25 February 2015 / Accepted: 16 March 2015 / Published: 28 April 2015

In this study we present an azoether dye, 4-[(4-chlorobenzyl)oxy]-4'-chloro-3,5-dimethyl-azobenzene (CDAB), obtained by condensation of 4-chloromethyl chlorobenzene with 4-(4-chloro-phenylazo)-2,6-dimethyl-phenol using the Williamson etherification method, as a new inhibitor for corrosion of carbon steel in solution of 0.15 M NaCl/water/dioxane (WDS). Successive electrochemical measurements such as: potentiodynamic polarization, general corrosion and electrochemical impedance spectroscopy (EIS) were performed, in order to study the contribution of CDAB to the formation of the protective layer on the surface of carbon steel in WDS. The CDAB's electrochemical instability and the adsorption of its molecules on carbon steel surface were discussed according to the data obtained from UV-Vis spectrophotometry and from Temkin adsorption isotherm. By corroborating all the data, we assume that the formation of the protective layer on the surface of carbon steel corroded in WDS containing CDAB is attributed to a synergistic contribution resulting from: the pure adsorption of CDAB inhibitor; the "bridged chloride" formation between CDAB molecules and carbon steel surface; the pure adsorption of other organic compounds resulting from the CDAB electrochemical decomposition such as 2,6-dimethyl-benzoquinone and chlorobenzene; the dioxane adsorption that can enhance the action of CDAB as a corrosion inhibitor for carbon steel in WDS. The adsorption of CDAB on carbon steel surface is the primordial process that prevails other processes and it was manifested even during the electrode prepolarization at open circuit. The optical microscopy images attest a different surface morphology for the carbon steel corroded in WDS dealt with CDAB compared to that shown in the absence of CDAB.

Keywords: corrosion inhibition; 4-[(4-chlorobenzyl)oxy]-4'-chloro-3,5-dimethyl-azobenzene; electrochemical measurements; UV-Vis spectrophotometry; action mechanism

1. INTRODUCTION

The electrochemical behaviour of alloys and metals in organic solvents or hydro-organic solutions has received greater attention over the past years. Organic solvents present specific effects which lead to major modifications of corrosion phenomena on metallic surfaces and thus, they influence the corrosion rate. The corrosion behaviour of metals in hydro-organic solutions has been studied because of their use in automotive engine industry, pipe, pipeline and transport containers. As compared with water, the corrosion mechanism in organic media with low dielectric constants was stated as purely chemical, while in aqueous-organic media, both water and the organic solvent may be a stimulator or an inhibitor [1-5].

Pitting corrosion of stainless steel was studied in 0.1 M KCl/water-organic solvent mixture (water-methanol, -ethanol, -isopropanol, -2-ethoxyethanol, -ethylene glycol, -acetonitrile). The organic solvents inhibited the pitting corrosion by increasing the viscosity of the medium, which leads to a decrease in the diffusion coefficients for the corrosion products out of the pit; the corrosion inhibition increases with concentration from 0.0 to 80 vol.% of organic solvent [6-8]. Stress corrosion cracking susceptibility of carbon steel in simulated fuel grade ethanol was investigated by electrochemical measurements in aerated and deaerated ethanol [9-15]. The presence of chloride ions is required for cracking occurrence, but is not the controlling factor of crack growth. Also, water, acetic acid, chloride anions, and the presence of oxygen plays an important role in general or localized corrosion of carbon steel in simulated fuel grade ethanol [16-18].

The decrease in organic solvent component concentration induces pitting and metal loss, while alkaline conditions inhibit both localized and uniform corrosion. Cathodic reaction of oxygen and hydrogen have been investigated on carbon steel in simulated fuel grade ethanol using cathodic potentiodynamic polarization and electrochemical impedance spectroscopy [19-21]. The presence of oxygen, even at low concentrations, lead to oxygen reduction, while hydrogen reduction, from acetic acid, ethanol and water, needs a very high cathodic overpotential in deaerated solution, which can be hardly achieved in normal corrosion process.

Repassivation of X65 carbon steel in fuel grade ethanol occurs faster in aqueous environments compared to organic solvent media [22-24]. In deaerated fuel ethanol, or aerated fuel ethanol containing water or chloride anions, pitting and localized corrosion occurred preferentially in the region where the film had been removed by scratching. Self-organized pores are formed on 316 stainless steel by electrochemical treatment in ethylene glycol containing perchloric acid [25]. The growth rate of pores (diameter and depth) was higher in the presence of water. Corrosion behaviour of 430 type stainless steel in hydrochloric acid solutions of methanol, ethanol and their binary mixture with water has been investigated by potentiostatic polarization and weight loss method [26, 27]. It was found that the corrosion rate was affected by the physico-chemical properties of the media such as: viscosity, solvation degree, molar volume contraction, proton availability and dielectric constant.

Microstructural and corrosion studies of 9Cr-1Mo steel in methanol containing different concentrations of sulphuric, hydrochloric acid and their mixtures under potentiostatic and potentiodynamic techniques has been studied [28]. The presence of water and acids in many of the organic solvents is reported to have encouraged the corrosion of many metals. Systematic investigation

have been carried out on electrochemical behaviour of mild steel in dimethyl sulfoxide containing various concentrations of hydrochloric acid [29] in presence of tetra ethyl ammonium chloride as supporting electrolyte.

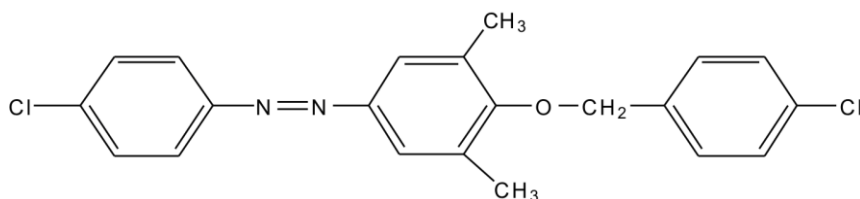
Some researchers report problems associated with the corrosion of: Al-Si, Cr-steel, C-steel, Al, Cu and Sn in 20 % bioethanol – 80 % gasoline [30-36], Cu in water-ethanol, -ethylene glycole, -glycerol, -dimethyl sulfoxide and dioxane [37], Al-Si-Cu-Fe(Zn) and Al-Si-Cu-Mg in ethanol solution containing water and acetic acid [38, 39] and titanium in non-aqueous, non-alcoholic solvents such as ethyl ether, acetic acid and acid anhydride [40].

This study presents the investigation of 4-[(4-chlorobenzyl)oxy]-4'-chloro-3,5-dimethyl-azobenzene (CDAB) as corrosion inhibitor for carbon steel in 0.15 M NaCl / water-dioxane solvent mixture (WDS) using electrochemical measurements associated with UV-Vis spectrophotometry and optical microscopy. The choice of this compound as corrosion inhibitor is based on: it is easily to be synthesized [41]; it was reported as antimicrobial agent, inhibiting the growth of some bacteria [42]; it is easily soluble in dioxane; his molecules have oxygen and nitrogen atoms, as active centers.

2. MATERIALS AND METHODS

2.1. Materials

The carbon steel plates (area of 1.0 cm²) with the following composition (weight %): C=0.15%; Si=0.035%; Mn=0.4%; Cr=0.3%; Ni=0.3%; Fe in balance, were used in order to investigate the corrosion process in 0.15 M NaCl/water-dioxane solution, in ratio 1:1 (volume) blank (WDS) and in the same electrolyte containing different concentrations of 4-[(4-chlorobenzyl)oxy]-4'-chloro-3,5-dimethyl-azobenzene (CDAB): 0.3 mM; 0.5 mM; 0.8 mM; 1.0 mM. The samples were mechanically polished with emery paper, degreased with acetone and dried. The synthesis of CDAB was performed by condensation of 4-chloromethyl chlorobenzene with 4-(4-chloro-phenylazo)-2,6-dimethyl-phenol using the Williamson etherification method, this being reported in our previous study [41]. Its spectral characterization by IR and UV-vis techniques [41] and *NMR* and *MS* [42] were carried out and discussed detailed [41, 42]. CDAB was screened for its antibacterial activity against *Staphylococcus aureus*, *Streptococcus pyogenes*, *Escherichia coli*, *Pseudomonas aeruginosa*, *Proteus vulgaris* and for its antifungal activity against *Candida albicans* by disk diffusion method, using the Mueller-Hinton culture medium [42]. All reagents were obtained from Fluka. The molecular structure and the UV-Vis spectrum of CDAB (concentration in dioxane of 0.1 mM) are illustrated in Fig. 1.



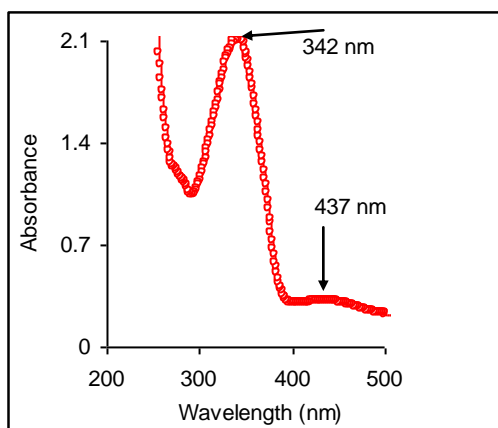


Figure 1. UV-Vis spectrum of 0.1 mM CDAB in dioxane

2.2. Electrochemical measurements

The anodic and cathodic polarization curves were recorded, with a scan rate of 1 mV/sec, for the carbon steel corrosion in blank WDS and in WDS containing various concentration of CDAB, in order to determine the corrosion rate expressed as corrosion current density (i_{corr}). Prior the corrosion measurements, the electrodes were maintained a time of 4.0 min at open circuit, at room temperature.

After 4.0 min., relaxation time of the electrodes at open circuit, the polarization resistance (R_p) values were also evaluated at different times: 72 s; 144 s; 216 s; 288 s; 360 s; 432 s; 504 s, using the general corrosion program, as an option to investigate the stability of the surface protective layer formed on carbon steel, after potentiodynamic polarization by calculation of degree of coverage (θ) and by the simulation its variation in time.

The electrochemical impedance spectroscopy (EIS) presented as Nyquist spectra for carbon steel corroded in WDS, in the absence and in the presence of CDAB, was performed in the frequency range of 10^5 Hz - 10^{-1} Hz, with amplitude of 10 mV. The electrochemical impedance measurements were carried out after both, potentiodynamic polarization and general corrosion, and the same relaxation time of the electrodes at open circuit of 4.0 min., there was.

A VoltaLab 40 potentiostat/galvanostat with VoltaMaster 4 software was used, in order to perform all electrochemical measurements of carbon steel in blank WDS and in WDS containing CDAB. For each test, it was used a glass corrosion cell with three electrodes: a platinum auxiliary electrode, a saturated Ag/AgCl_{sat}, as reference electrode (area of 1.0 cm²) and carbon steel plates (area of 1.0 cm²), as working electrodes.

2.3. UV-Vis spectrophotometry

The blank solution and inhibitor solutions containing various concentration of CDAB: 0.3 mM; 0.5 mM; 0.8 mM; 1.0 mM were analyzed before and after corrosion by UV-Vis spectrophotometry recording the UV-Vis spectra in wavelength range between 800 nm and 200 nm using a Varian-Cary 50 spectrophotometer with CaryWin software. Operating mode: the solutions were placed in the UV-VIS

beam and the scans of the absorbance in function of the wavelength were obtained in the same time with the analysis report for each sample separately. Also, the calibration curve was drawn by reading the absorbance values corresponding to some known concentrations of inhibitor: 0.1 mM; 0.3 mM; 0.5 mM; 0.7 mM; 0.9 mM, in order to detect the concentration of CDAB after the corrosion process.

2.4. Optical microscopy

An optical Euromex microscope with Canon camera and included ZoomBrowser - EOS Digital software was used to examine the carbon steel surface before and after corrosion.

3. RESULTS AND DISCUSSION

3.1. Potentiodynamic polarization

To estimate the effect of CDAB on carbon steel corrosion in WDS, the potentiodynamic curves were recorded in the absence and in the presence of CDAB with a scan rate of 1.0 mV s^{-1} , after the electrode prepolarization at open circuit for 4.0 min., at room temperature (Fig. 2).

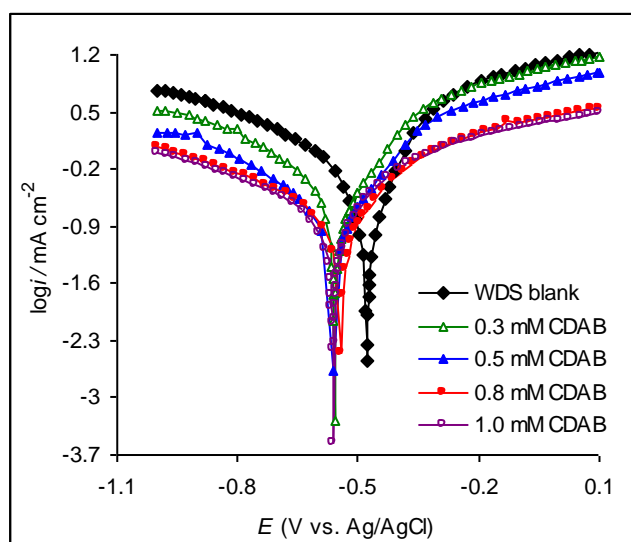


Figure 2. Anodic and cathodic polarization curves obtained for carbon steel corroded in WDS blank and in WDS containing various concentrations of CDAB, at room temperature.

The addition of CDAB in WDS leads to the displacement of potentiodynamic curves in regions of lower current than that corresponding to the carbon steel corroded in blank WDS. From Fig. 2 it can be seen that the CDAB presence in WDS shifts the corrosion potential (E_{corr}) to more negative values with a significant effect on both anodic and cathodic processes. These clues mention that: (i) the addition of CDAB in WDS leads to the diminishing of the corrosion current, but it can not be revealed an action mechanism of the inhibitor; (ii) the both shape and the position of polarization curves show

that the cathodic reaction is reduced starting with low concentrations of CDAB in this environment; (iii) the manner of anodic process inhibition is dependent on the anode potential, as follows:

- beginning with the potential value of -0.29 V, the characteristic of the polarization curve recorded for the carbon steel in WDS containing 0.3 mM CDAB is unchanged, this being overlapped on the polarization curve obtained in WDS blank, being understood that the dissolution reaction prevails the inhibition one;

- from the concentration value of 0.5 mM until 1.0 mM, a film occurrence on the carbon steel surface is possible at the potential values higher than -0.42 V. The composition of this film is not predictable only from these measurements, but the synergy between dioxane and CDAB adsorption on carbon steel surface may be discussed as possible phenomenon.

These arguments predict that the addition of CDAB in WDS inhibits both processes, behaving like a mixed inhibitor [43, 45-55], but predominantly cathodic.

As a consequence, the corrosion current decreases while the inhibition efficiency (*IE*) increases with increasing the CDAB concentration in WDS (Table 1).

By plotting the $E = f(\log i)$, at overvoltage (η) values higher than 52 mV, for the anodic process and overvoltage values lower than of -52 mV corresponding to the cathodic process, straight lines is obtained which are described by Tafel equations [44, 45]. Thus, the corrosion current density (i_{corr}) was determined from the intersection of Tafel lines, at corrosion potential (E_{corr}), while the anodic and cathodic Tafel slopes (ba & bc) was deduced as $[dE/d(\log i)]_{E \gg E_{\text{corr}}}$, this meaning $[d\eta/d\log i]_{\eta \geq 52}$, from anodic Tafel equation and $[d\eta/d\log i]_{\eta \leq -52}$, from cathodic Tafel equation, respectively [44, 45].

As shown in Table 1, the presence CDAB in WDS lowers i_{corr} and different values of Tafel slopes have resulted compared to those obtained in its absence. This could indicate that the inhibition process takes place by blocking the active sites on the surface of carbon steel [50-55], slowing the iron oxidation process and by reducing the cathodic reactions on the whole. This can be interpreted as an effect of some changes at the metal/electrolyte interface, which have occurred by the replacement of WDS molecules with CDAB molecules, or with the molecules of the compounds resulted by the inhibitor electrochemical degradation.

To calculate the electrochemical parameters such us: the corrosion potential (E_{corr}), the corrosion current density (i_{corr}), the anodic and cathodic Tafel slopes (ba & bc) the VoltaMaster4 software was used. The inhibition efficiency (*IE*) values depending on the CDAB concentration (*C*-CDAB) was determined from potentiodynamic polarization in accordance with the equation written below, Eq. 1 [45-49]:

$$IE = \frac{i_{\text{corr}}^{\circ} - i_{\text{corr}}}{i_{\text{corr}}^{\circ}} \times 100 \quad (1)$$

where i_{corr}° and i_{corr} represents the corrosion current density of carbon steel corroded in blank WDS and in WDS containing CDAB, respectively.

Table 1. Electrochemical parameters and inhibition efficiency (*IE*) calculated from potentiodynamic curves obtained for the carbon steel corrosion in blank WDS and in WDS containing various concentrations of CDAB

C-CDAB/ mmol L ⁻¹	E _{corr} / mV vs. Ag/AgCl	i _{corr} / mA cm ⁻²	b _a / mV dec ⁻¹	b _c / mV dec ⁻¹	IE/ %
0	-478	0.653	90	-366	0
0.3	-559	0.267	105	-331	59.1
0.5	-564	0.211	109	-274	67.8
0.8	-541	0.138	119	-262	78.9
1.0	-560	0.112	118	-252	82.8

3.2. General corrosion

In order to evaluate the adherence and the stability of the film that was formed on carbon steel surface, the general corrosion was carried out after potentiodynamic polarization, by determination of polarization resistance values (*R_p*) at different times: 72 s; 144 s; 216 s; 288 s; 360 s; 432 s; 504 s followed by the calculation of surface coverage degree (*θ*) using the Eq. 2 [50].

$$\theta = \left(\frac{R_p - R_p^0}{R_p} \right) \tag{2}$$

where *R_p* and *R_p⁰* represent the polarization resistance to a time moment in the presence and in the absence of CDAB, respectively.

The variation of both, the polarization resistance values (*R_p*) and surface coverage degree (*θ*) over time may be observed in Fig. 3.

From Fig. 3a it is seen that, the increase of *R_p* value in time becomes more and more obvious with the increasing of CDAB concentration. This indicates that CDAB makes an important contribution to film formation and to its stability on substrate, in time.

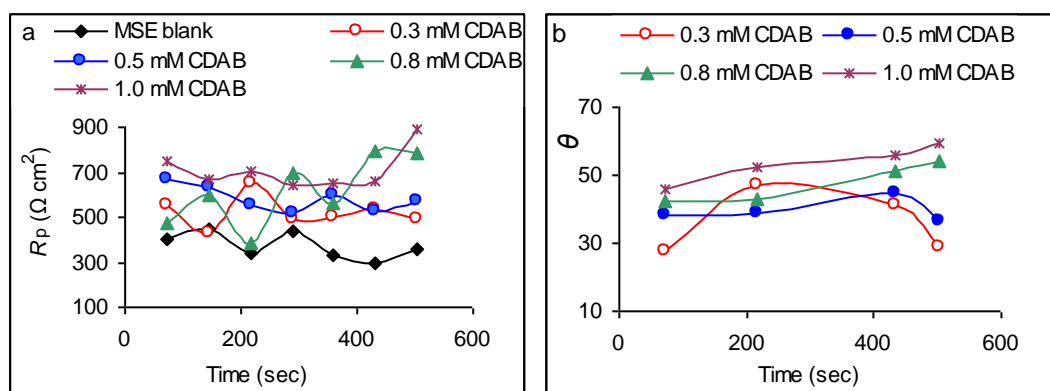


Figure 3. The variation of polarization resistance in time for carbon steel corroded in WDS blank and in WDS containing CDAB (a); degrees of surface coverage over time, involving the contribution of CDAB to protective layer formation (b).

The same trend is also observed for degree of surface coverage (θ), excepting the first concentration of 0.3 mM CDAB that mark a decrease of θ values, by forming a large shoulder, with a maximum at 216 s (Fig. 3b).

This could be explained by the occurrence of some anodic areas on the carbon steel surface where corrosion processes are pretty intense [50], inducing instability and permeability to inhibitor film [50], meaning that, the inhibitor concentration is too low to ensure the formation of a continuously and somewhat compact layer to protect the metal surface [50]. For concentrations higher than 0.5 mM CDAB, it is observed that θ values are stable reaching a value of 0.596 at 1.0 mM CDAB in WDS.

Consequently, IE reaches the values of 59.6%, this being smaller than that obtained from potentiodynamic polarization. This difference is predictable because in the given conditions, the inhibitor may follow several cycles of adsorption - desorption of its molecules, and/or another contribution to protective layer formation may be take in consideration, such as the appearance of new compounds resulted from CDAB electrochemical decomposition.

3.3. Electrochemical impedance spectroscopy (EIS)

To study the protective layer destruction, the EIS measurements for carbon steel were recorded in blank WDS and WDS containing various concentration of CDAB, after potentiodynamic polarization and general corrosion, the relaxation time of the electrodes, at open circuit, between measurements being of 4.0 minutes. Thus, the Nyquist diagram is presented in Fig. 4. From Fig. 4, it can be observed that the capacitive loop appears as a semicircle in Nyquist diagram being more pronounced with the increase in CDAB concentration. The impedance data of carbon steel corroded in WDS, without and with various CDAB concentrations were fitted using an equivalent circuit (inserted in Fig. 4) that involves R_s (solution resistance), CPE (constant phase element) and R_{ct} (charge transfer resistance) that is in parallel placed with CPE .

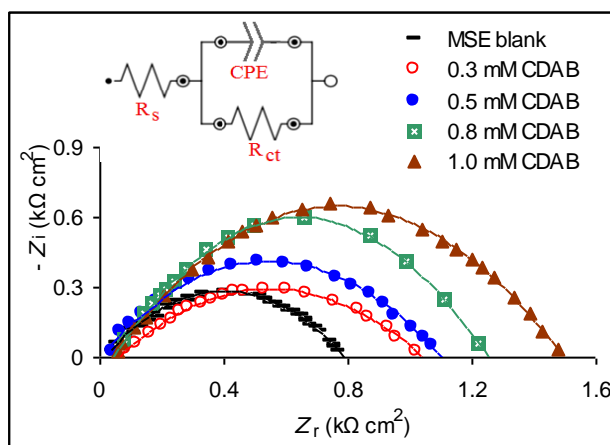


Figure 4. Equivalent circuit model and Nyquist diagram of carbon steel corroded in WDS blank and in WDS containing various concentrations of CDAB, after potentiodynamic polarization and general corrosion, at room temperature.

Thus, in Nyquist plots, the intersection of the capacitive loop with the real axis, at very low frequencies, represents the charge transfer resistance (R_{ct}), and the solution resistance (R_s) at very high frequencies [47, 52].

Similar curves were obtained for other inhibitors [45-52]. The inhibition efficiency (IE) was determined using the following expression, Eq. 3 [45-51]:

$$IE = \left(\frac{R_{ct} - R_{ct}^0}{R_{ct}} \right) \cdot 100 \quad (3)$$

where R_{ct} and R_{ct}^0 represent the charge transfer resistances in the presence and in the absence of CDAB.

The double layer capacitance (C_{dl}) was derived from frequency, at which the imaginary component of the impedance ($-Z_{imax}$) was maximal [46, 47, 51], using the relationship, Eq. 4 [46, 47, 51]:

$$f(-Z_{imax}) = \frac{1}{2\pi C_{dl} R_{ct}} \quad (4)$$

The impedance parameters derived from EIS measurements R_s , R_{ct} , C_{dl} and n were calculated using VoltaMaster 4 software with an error of ± 1 %, and these are listed in Table 2.

Table 2. Electrochemical parameters and inhibition efficiency (IE) derived from EIS for carbon steel corroded in WDS in the absence and in the presence of various concentrations of CDAB, after potentiodynamic polarization and general corrosion, at room temperature.

C-CDAB/ mmol L ⁻¹	R_s / Ω cm ²	C_{dl} / μ F cm ⁻²	n	R_{ct} / Ω cm ²	IE / %
0	0.037	55.95	0.798	748	0
0.3	0.082	22	0.84	1029	27.3
0.5	0.041	18.68	0.88	1089	31.3
0.8	0.06	17.34	0.91	1254	40.3
1.0	0.061	6.45	0.968	1516	50.6

By inspecting the data from Table 2 it can be observed that the addition of CDAB in WDS increases R_{ct} and decreases C_{dl} and consequently IE improves, reaching a maximum value of 50.6 %, at 1.0 mM of CDAB in WDS. The decrease in C_{dl} could be attributed to the decrease in local dielectric constant and/or an increase in the thickness of the electrical double layer [51, 52], signifying that CDAB molecules contribute to the stability of protective layer adsorbed on carbon steel.

Both the degree of surface coverage and inhibition efficiency are lower than in the cases discussed above, which may be attributed to either partial desorption of inhibitor and/or its electrochemical instability. High polarization resistance obtained by EIS confirms the formation of a protective layer whose development mechanism could be attributed to major changes in the electrical double layer due to: the pure adsorption of CDAB molecules on the carbon steel surface; the pure adsorption of other compounds resulting from the decomposition thereof; the appearance of a layer

composed of iron corrosion products, with insertion of some organic molecules like: dioxane, CDAB and other resulting from CDAB electrochemical degradation.

3.4. Action mechanism of CDAB

To propose an action mechanism of CDAB as corrosion inhibitor for carbon steel corrosion in WDS, the estimation of its possibilities to link on the surface is mandatory, in order to explain the formation of a protective film [46]. To study the CDAB electrochemical stability, as well as its adsorption capacity on carbon steel surface, the UV-Vis scans of blank WDS and WDS containing CDAB, before and after corrosion processes, were performed.

Figs. 5a-b illustrate the UV-Vis scans obtained for CDAB solutions in WDS with the following concentrations: 0.3 mM; 0.5 mM; 0.8 mM; 1.0 mM, before and after all electrochemical measurements, at room temperature. UV-Vis spectra showed K bands due to the conjugated system Ar-N=N-Ar at 342-370 nm, and R-type bands due to the chromophore azo group -N=N-, at 435-440 nm [41]. Thus, the calibration curve of CDAB was performed for the intense band at 437 nm (Fig. 5c), in order to calculate the concentration values after corrosion process.

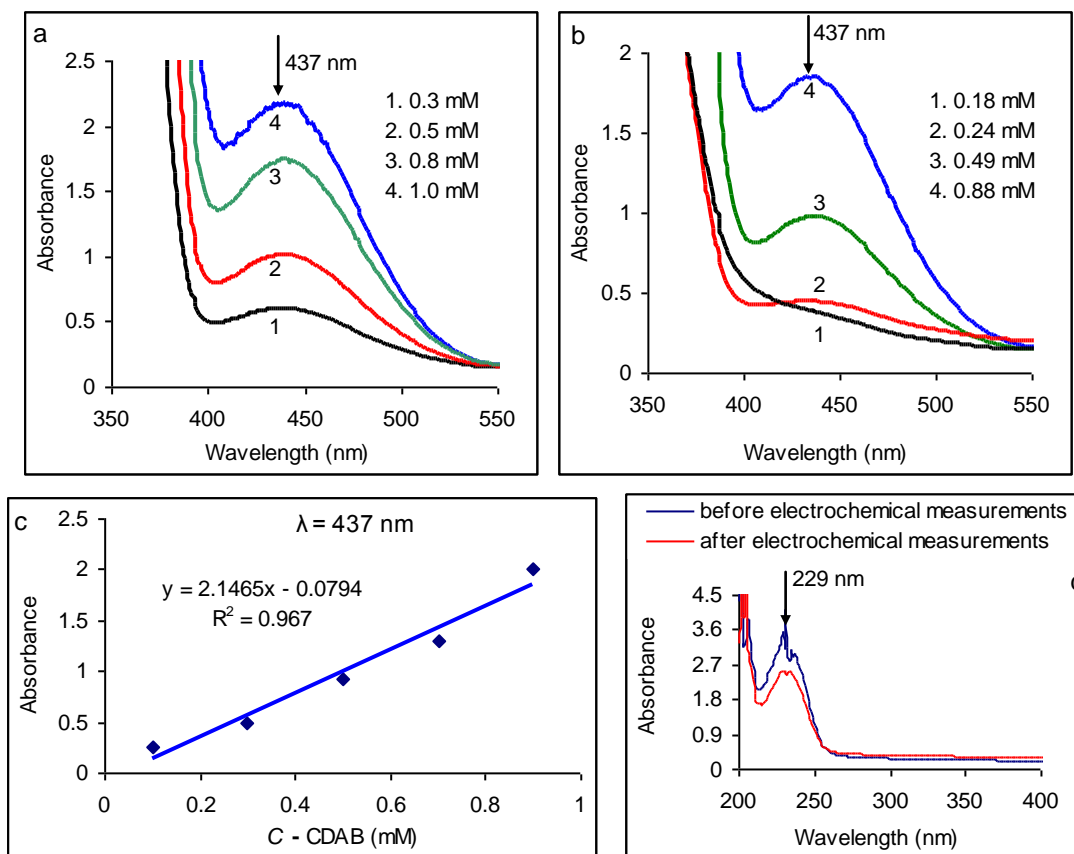
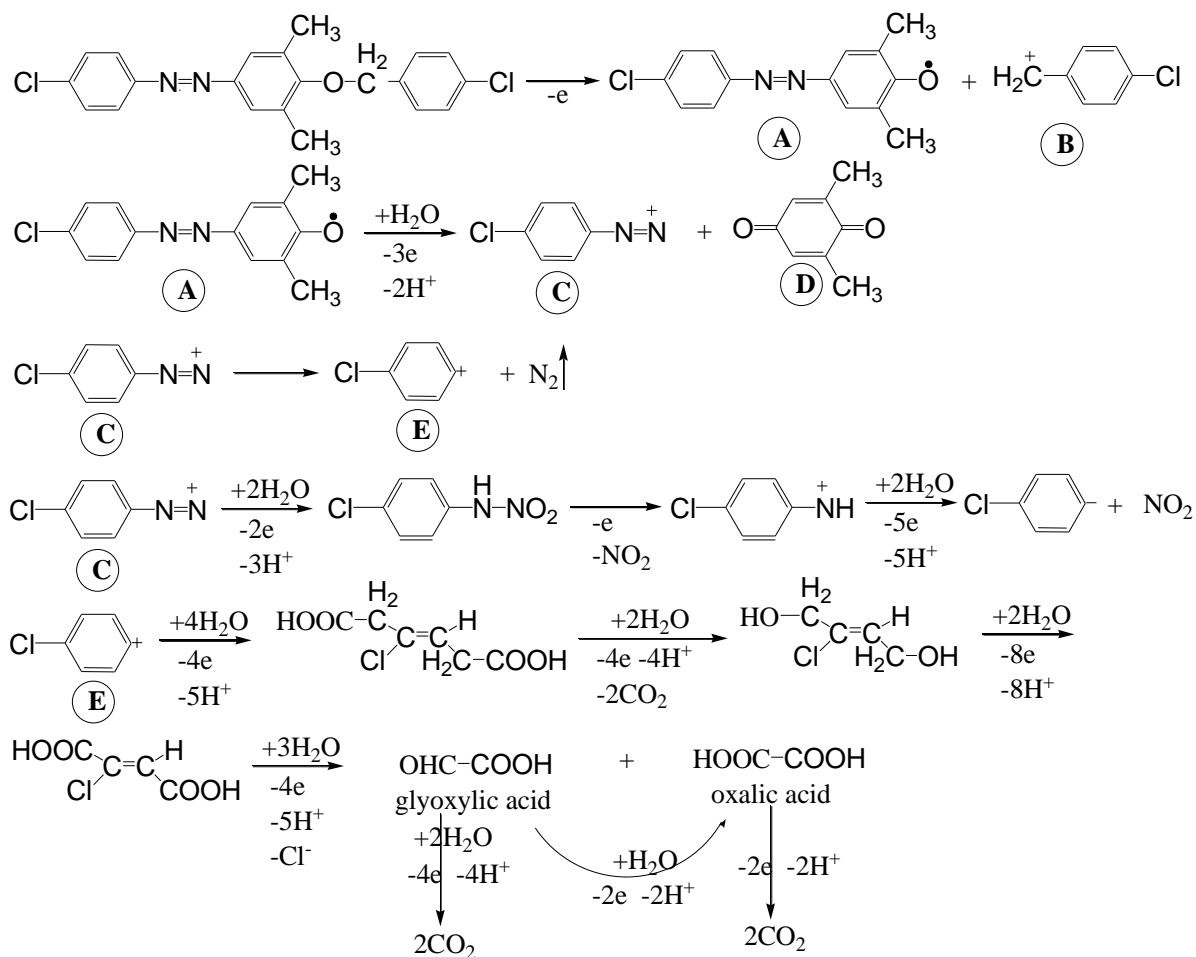
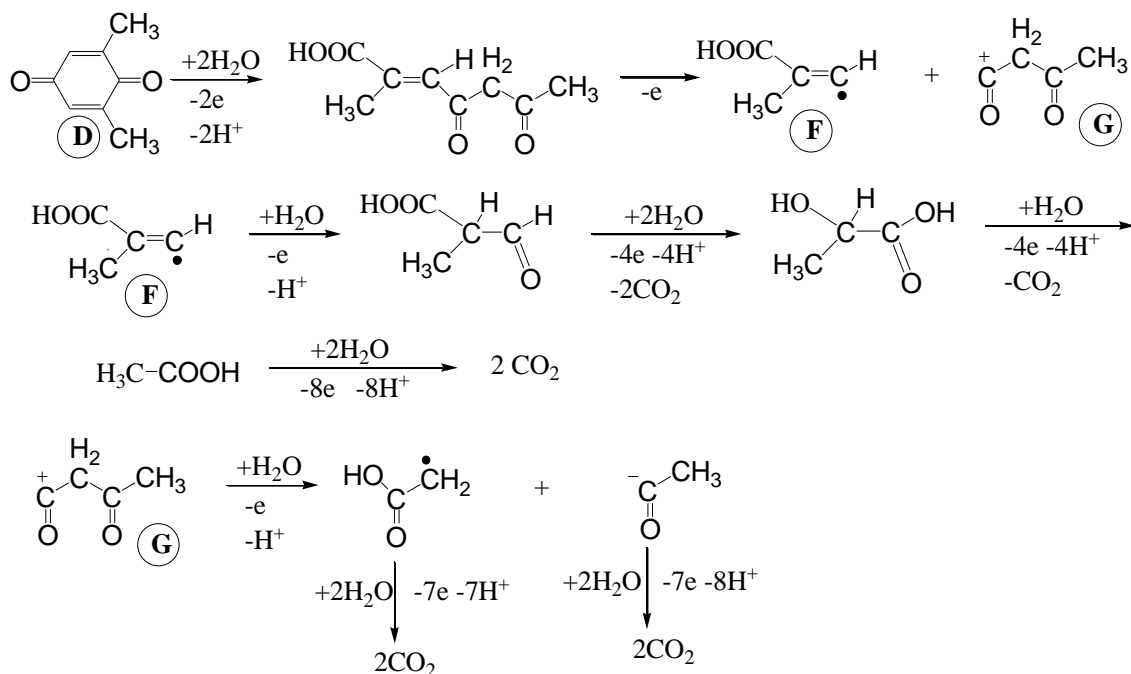


Figure 5. UV-Vis spectra recorded for the carbon steel in WDS containing different concentrations of CDAB; a - before electrochemical measurements; b - after the corrosion tests; c - CDAB calibration chart in WDS; d - WDS blank (dioxane at $\lambda=229 \text{ nm}$)

The WDS blank was analyzed recording the dioxane absorbance prior and after corrosion process takes place (Fig. 5d), being obvious that the dioxane concentration decreases, after electrochemical measurements. This suggests the dioxane transformation; it is difficult to explain from only the UV-Vis data, but it can be intuited its adsorption on carbon steel surface as primary process, its decomposition and/or its possible reactions with other compounds from environment, as a secondary phenomena. Fig. 5b shows that after the corrosion process, CDAB absorbance decreases without altering the wavelength of adsorption maximum, and consequently the inhibitor concentration in corrosive medium follows the same trend. Thus, as shown in Fig. 5b, after the corrosion process, all concentrations of CDAB were diminished, inducing the hypothesis that, during electrochemical tests, a part of CDAB was decomposed. Consequently, the decomposition mechanism of CDAB was proposed, as follows (Scheme 1). The azoether molecule may undergo cleavage of the O-CH₂ bond to give the radical **A** and the carbocation **B** (4-chlorobenzyl cation). In a subsequent fragmentation, from **A**, the cation **C** and one molecule of 2,6-dimethyl-benzoquinone (**D**) may be obtained. Cl-C₆H₄-N₂⁺ (**C**) can be transformed in two ways: (1) it loses N₂ and generates 4-chlorophenyl cation (**E**); (2) in solution, it converted in *N*-nitro-(4-chloroaniline) and 4-chlorophenyl cation which is finally transformed in chlorobenzene and NO₂. 2,6-dimethyl-benzoquinone (**D**) is transformed in two intermediates: radical **F** and carbocation **G**, that can support further reactions, being finally degraded to H₂O and CO₂.





Scheme 1. The proposed electrochemical decomposition mechanism of CDAB

We assume that the overall process of electrochemical decomposition yields 2,6-dimethylbenzoquinone and chlorobenzene as organic products and H_2O and CO_2 , as final inorganic compounds.

By corroborating all the data we assume that the formation of the protective layer on the surface of carbon steel corroded in WDS containing CDAB is attributed to a synergistic contribution resulting from: (i) the CDAB pure adsorption by interactions between the non-bonding electrons of the nitrogen atoms from the azo group and from the oxygen atom of the side chain with the vacant “*d*” orbital from iron; (ii) the “bridged chloride” [52] formation between CDAB molecules and carbon steel surface represents, also, other possibility of inhibitor binding on substrate; (iii) pure adsorption of other organic compounds resulting from the CDAB breakdown like 2,6-dimethylbenzoquinone and chlorobenzene (see Scheme 1); (iv) the dioxane adsorption that can enhance the action of CDAB as a corrosion inhibitor for carbon steel in WDS; (v) the adsorption of CDAB on carbon steel surface which is the primordial process that prevails other processes, being manifested it even during the electrode prepolarization at open circuit, obviously taking into account the enhancer effect of dioxane.

3.5. Adsorption isotherm

Taking into account the above discussed aspects, we have decided to evaluate the quantitative adsorption of CDAB after each electrochemical measurement, in order to discuss the evolution of the equilibrium constant of adsorption-desorption (K) and standard free energy of adsorption (ΔG_{ads}^0), because the surface protective layer is subjected to change during each measurement.

Thus, the variation of surface coverage degree (θ) depending on the concentration of inhibitor (C-CDAB) has been plotted. As shown in Fig. 6a, a logarithmic function has fitted the experimental data, so the graphical representation of $\theta = f(\ln C\text{-CDAB})$ will illustrate a straight line [46].

Consequently, as Fig. 6b indicates, the adsorption model that can be adopted in such a case is represented by the Temkin isotherm [45, 46, 53-55], that may be expressed by Eq. 5 [45, 46, 53-55].

$$\theta = \frac{I}{f} \cdot \ln K + \frac{I}{f} \cdot \ln C \tag{5}$$

where C is the concentration (mol L⁻¹) of CDAB inhibitor in the bulk electrolyte, θ is the degree of surface coverage ($\theta = IE/100$), K is the adsorption-desorption equilibrium constant and f is the heterogeneous factor of metal surface, representing the number of surface active sites occupied by one inhibitor molecule.

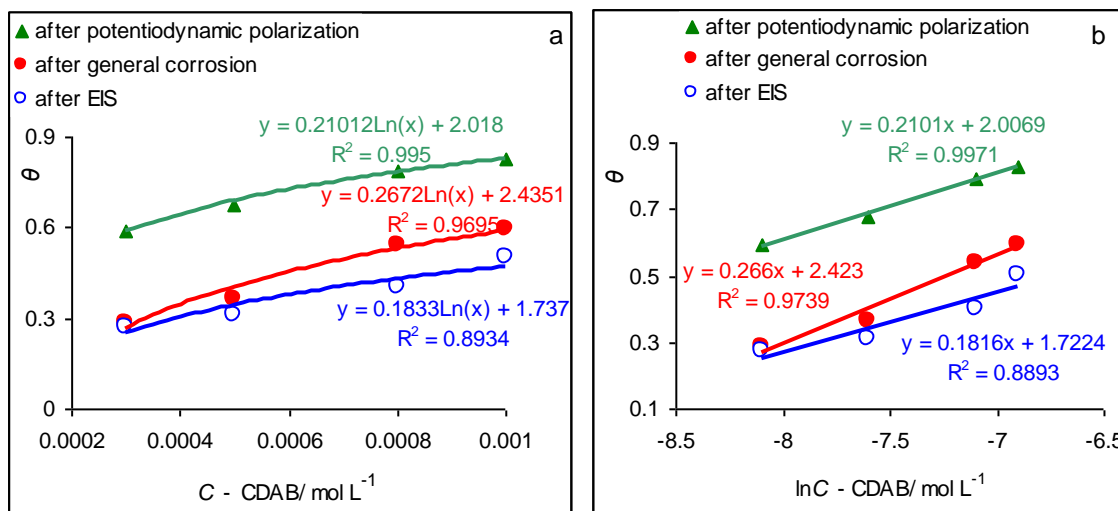


Figure 6. The variation of degree of surface coverage (θ) over CDAB concentration (a); Temkin adsorption isotherm obtained for carbon steel corroded in WDS without and with various concentrations of CDAB, at room temperature (b).

After all electrochemical measurements, straight lines relationships were obtained with regression coefficient (R^2) reaching values between 0.89 and 0.99, these being more or less close to unity, indicating the validity of Temkin model for the adsorption of CDAB molecules on carbon steel surface (see equations inserted in Fig. 6b). The difference between these values was expected due to transformations which took place at metal/electrolyte interface and to the changes occurred in the electrical double layer. These may disturb the adsorption process, but the adsorption mechanism is not affected. The slopes of the lines are equal to I/f and the intersections from which the K values were calculated are represented by $[(1/f) \cdot \ln K]$ [45, 49, 53-55]. The equilibrium constant of adsorption-desorption (K) was used to calculate the free energy of adsorption (ΔG^0_{ads}) using Eq.6 [45-49, 53-55]:

$$K = \frac{I}{55.5} \exp \left(- \frac{\Delta G^0_{ads}}{R \cdot T} \right) \tag{6}$$

where R is the universal gas constant (8.31 J mol⁻¹ K⁻¹), T is the temperature (K) and 55.5 is the molar concentration of water in the solution.

Knowing that 1 joule = 6.24×10^{18} electron volts (eV), and that 6.023×10^{23} is Avogadro number, the binding energy (BE) was also calculated for the anchoring of CDAB molecules on surface, using the following relationship, Eq. 7 [50, 55].

$$BE = \left(\frac{\Delta G_{\text{ads}}^{\circ} \cdot 6.24 \cdot 10^{18}}{6.023 \cdot 10^{23}} \right) \quad (7)$$

The thermodynamic parameters for the adsorption of CDAB on carbon steel surface in WDS according to Temkin adsorption isotherm are presented in Table 3.

Table 3. The adsorption parameters of CDAB on carbon steel surface in WDS, at room temperature

Electrochemical Measurement	Parameters					
	$1/f$	f	$(\ln K)/f$	$\ln K$	$\Delta G_{\text{ads}}^{\circ}/\text{kJ mol}^{-1}$	BE/eV
by potentiodynamic polarization	0.2101	4.76	2.0069	9.53	-33.55	0.348
by general corrosion	0.266	3.76	2.423	9.11	-32.46	0.336
by EIS	0.1816	5.5	1.7224	9.47	-33.36	0.345

The negative value obtained for $\Delta G_{\text{ads}}^{\circ}$ indicates a spontaneous adsorption of CDAB molecules and usually characterizes their interaction with the carbon steel surface surface [43-53]. Knowing that the value of $(-40 \text{ kJ mol}^{-1})$ for $\Delta G_{\text{ads}}^{\circ}$ is usually accepted as a threshold value between chemical and physical adsorption [45-55], the values which were obtained in our study (around of $-33.0 \text{ kJ mol}^{-1}$) demonstrate a moderate adsorption of CDAB molecules on carbon steel surface. This involve both chemical and physical adsorption mechanism, due to: interactions between the non-bonding electrons of the nitrogen atoms from the azo group and from the oxygen atom of the lateral chain with the vacant “ d ” orbital from iron and “bridged chloride” formation between CDAB molecules and carbon steel surface. Thus, the assumptions stated under paragraph 3.4 are confirmed.

3.6. Optical microscopy

The surface morphology of carbon steel before (Fig. 7a) and after corrosion (Fig. 7, from b to f) was examined by optical microscopy. In the case of WDS blank a large number of corrosion spots is observed on the carbon steel surface (b). For the CDAB concentration of 0.5 mM (d) the protective layer is more nuanced than that was formed at the inhibitor concentration of 0.3 mM CDAB (c). For 0.8 mM (e) and 1.0 mM (f) concentration of CDAB, there is a completely coated surface, and it could be associated to a protective layer composed of: iron corrosion products, inserted inhibitor molecules and of other compounds which were obtained by electrochemical decomposition of CDAB in WDS. The formation of a thin film due to a pure adsorption of the inhibitor on the surface is difficult to be identifiable, but the uniformity of the coating is obvious.

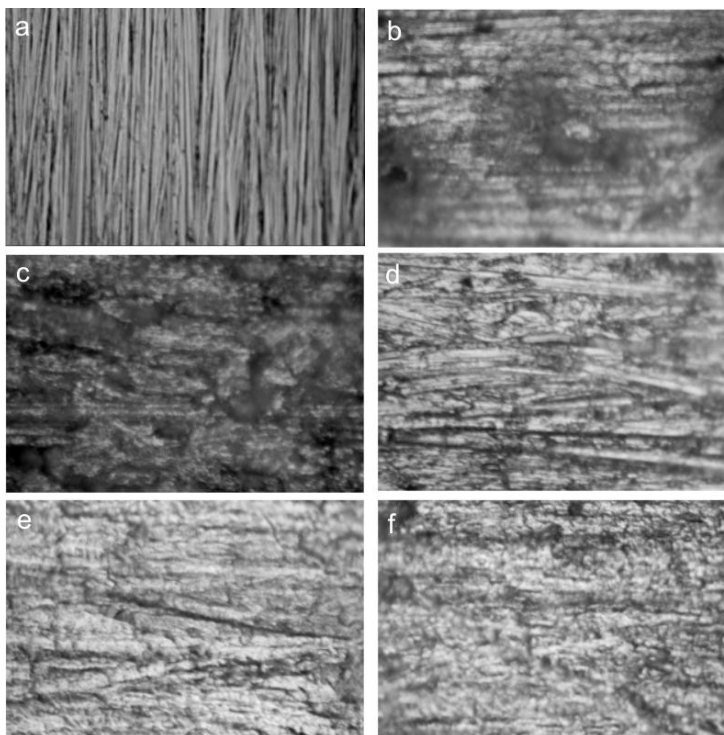


Figure 7. The microscopic images of the carbon steel surface: prior to the corrosion tests performing (a); after the carbon steel corrosion in WDS blank (b) and in WDS containing various concentrations of CDAB: 0.3 mM (c); 0.5 mM (d); 0.8 mM (e); 1.0mM (f).

4. CONCLUSIONS

Electrochemical behaviour of 4-[(4-chlorobenzyl)oxy]-4'-chloro-3,5-dimethyl-azobenzene (CDAB) was studied in order to investigate it as corrosion inhibitor in water-dioxane organic solvent mixture containing 0.15 M NaCl (WDS).

The electrochemical measurements were successively performed as follows: potentiodynamic polarization, general corrosion and electrochemical impedance spectroscopy (EIS) for the comparative discussion of electrochemical parameters and the mechanism of initiation, development and stability of the protective layer formed on the carbon steel surface in WDS. As associative methods, UV-Vis spectrophotometry and optical microscopy were used.

By corroborating all the data, it can be concluded that CDAB behaves as corrosion inhibitor for carbon steel in WDS, having inhibition efficiency (*IE*) of 82.8%, at 1.0 mM concentration, calculated after potentiodynamic polarization. The *IE* reaches the smaller values after general corrosion and EIS than that was obtained from potentiodynamic polarization suggesting that the inhibitor may follow several cycles of adsorption - desorption of its molecules, and/or another contribution to protective layer formation may be take in consideration, such as the occurrence of new compounds resulted from CDAB electrochemical degradation. Moreover, the CDAB mechanism of decomposition was proposed.

The action mechanism of CDAB as corrosion inhibitor of carbon steel in WDS was discussed by reporting to the data obtained from electrochemical tests and UV-Vis spectrophotometry in

association with optical microscopy, concluding that, the protective surface layer is composed of: iron corrosion products, the inhibitor molecules and other compounds which were obtained by electrochemical decomposition of CDAB in WDS.

The adsorption of CDAB on carbon steel surface is the primordial process that prevails other processes. This process takes place even during the electrode prepolarization at open circuit, obviously taking into account the enhancer effect of dioxane.

The experimental data were fitted using Temkin adsorption isotherm that indicated a moderate adsorption of CDAB molecules on carbon steel surface. This involves both chemical and physical adsorption mechanisms, due to: interactions between the non-bonding electrons of the nitrogen atoms from the azo group and from the oxygen atom of the side chain with the vacant “*d*” orbital from iron and “bridged chloride” formation between CDAB molecules and carbon steel surface.

ACKNOWLEDGEMENTS

This work was partially supported by the grant number 39C/27.01.2014 /2014, awarded in the internal grant competition of the University of Craiova.

References

1. A. Kriaa, N. Hamdi, K. Jbali and M. Tzinmann, *Corros. Sci.*, 51 (2009) 668.
2. V.V. Ekilik and V.P. Grigor`ev, *Prot. Met.*, 38 (2002) 124.
3. R.B. Rastogi, M.M. Singh, K. Singh and M. Yadav, *Port. Electrochim. Acta*, 22 (2005) 315.
4. R.B. Rastogi, M.M. Singh, K. Singh and J.L. Maurya, *Bull. Electrochem.*, 22 (2006) 355.
5. S.K. Singh and A.K. Mukherjee, *J. Mater. Sci. Technol.*, 26 (2010) 264.
6. B.A. Abd-El-Nabey, N. Khalil, M.M. Eisa and H. Sadek, *Surf. Technol.*, 20 (1983) 209.
7. B.A. Abd-El-Nabey, N. Khalil and M.M. Eisa, *Surf. Technol.*, 22 (1984) 9.
8. C.A. Farina and U. Grassini, *Electrochim. Acta*, 32 (1987) 977.
9. X. Lou and P.M. Singh, *Electrochim. Acta*, 56 (2011) 1835.
10. Liu Cao, G.S. Frankel and N. Sridhar, *Electrochim. Acta*, 104 (2013) 255.
11. R. Singh, *Materials Performance*, 48 (2009) 53.
12. N. Sridhar, *Materials Performance*, 46 (2007) 18.
13. E. Torsner, *Corros. Eng. Sci. Technol.*, 45 (2010) 42.
14. N. Sridhar, K. Price, J. Buckingham and J. Dante, *Corros.*, 62 (2006) 687.
15. C.S. Brossia, E. Gileadi and R.G. Kelly, *Corros. Sci.*, 37 (1995) 1455.
16. X. Lou and P.M. Singh, *Corros. Sci.*, 52 (2010) 2303.
17. T. Ramgopal and S. Amancherla, *Corros.*, 61 (2005) 1136.
18. H.B. Shao, J.M. Wang, X.Y. Wang, J.Q. Zhang and C.N. Cao, *Electroch. Commun.*, 6 (2004) 6.
19. X. Lou and P.M. Singh, *Electrochim. Acta*, 56 (2011) 2312.
20. J. Banas, B. Stypula, K. Banas, J. Swiatowska-Mrowiecka, M. Starowicz and U. Lelek-Borkowska, *J. Solid State Electroch.*, 13 (2009) 1669.
21. J. Swiatowska-Mrowiecka and J. Banas, *Electrochim. Acta*, 50 (2005) 1829.
22. L.R. Goodman and P.M. Singh, *Corros. Sci.*, 65 (2012) 238.
23. X. Lou, D. Yang and P. Singh, *Corros.*, 65 (2009) 785.
24. X. Lou, D. Yang and P. Singh, *J. Electrochem. Soc.*, 157 (2010) C86.
25. H. Tsuchiya, T. Suzumura, Y. Terada and S. Fujimoto, *Electrochim. Acta*, 82 (2012) 333.
26. A.A. Khedr, I.Z. Selim, K.M. El-Sobki and O.S. Shehata, *J. Mater. Sci. Technol.*, 10 (1994) 411.
27. V.B. Singh and Monali Ray, *Int. J. Electrochem. Sci.*, 2 (2007) 329.

28. V.B. Singh and A. Gupta, *Indian J. Chem. Technol.*, 12 (2005) 347.
29. R.B. Rastogi, M.M. Singh, K. Singh and J.L. Maurya, *Portugaliae Electrochim. Acta*, 28 (2010) 359.
30. L.M. Baena, M. Gomez and J.A. Calderon, *Fuel*, 95 (2012) 320.
31. G.K. Pedraza-Basulto, A.M. Arizmendi-Morquecho, J.A. Cabral Miramontes, A. Borunda-Terrazas, A. Martinez-Villafane and J.G. Chacón-Nava, *Int. J. Electrochem. Sci.*, 8 (2013) 5421.
32. W. Aperador, J. Caballero-Gomez and A. Delgado, *Int. J. Electrochem. Sci.*, 8 (2013) 6154.
33. I.J. Park, Y.H. Yoo, J.G. Kim, D.H. Kwak and W.S. Ji, *Fuel*, 90 (2011) 633.
34. L. Kruger, F. Tuchscheerer, M. Mandel, S. Muller and S. Liebsch, *J. Mater. Sci.*, 47 (2012) 2798.
35. H. Jafari, M.H. Idris, A. Ourdjini, H. Rahimi and B. Ghobadian, *Mater. Corros.*, 61 (2010) 432.
36. A. Carreon-Alvarez, R.C. Valderrama, J.A. Martinez, A. Estrada-Vargas, S. Gomez-Salazar, M. Barcena-Soto and Norberto Casillas, *Int. J. Electrochem. Sci.*, 7 (2012) 7877.
37. M.A. Shaker and H.H. Abdel-Rahman, *American J. Appl. Sci.*, 4 (2007) 554.
38. G.L. Song and M. Liu, *Corros. Sci.*, 72 (2013) 73.
39. T. Kikuchi, Y. Hara, M. Sakairi, T. Yonezawa and A. Yamauchi, *Corros. Sci.*, 52 (2010) 1482.
40. S.P. Trasatti and E. Sivieri, *Mat. Chem. Phys.*, 92 (2005) 475.
41. S. Radu, A. Moanță and G. Rău, *Rev. Chim.*, 52 (2001) 619.
42. A. Moanță, G. Rău and S. Radu, *Rev. Chim.*, 58 (2007) 229.
43. A. Samide, B. Tutunaru, C. Negrila, I. Trandafir, A. Maxut, *Dig. J. Nanomater. Bios.*, 6 (2011) 663.
44. I.G. Murgulescu, O.M. Radovici, *Introducere in Chimie fizica, vol. IV, Electrochimie (Introduction in Physical Chemistry. Vol. 4: Electrochemistry)*, Publisher: Romanian Academy, Bucharest, 1986.
45. A. Moanță, A. Samide, C. Ionescu, B. Tutunaru, A. Dobritescu, A. Fruchier, V. Barragan-Montero, *Int. J. Electrochem. Sci.*, 8 (2013) 780.
46. A. Samide and B. Tutunaru, *Cent. Eur. J. Chem.*, 12 (2014) 901.
47. B. Zerga, A. Attayibat, M. Sfaira, M. Taleb, B. Hammouti, M. Ebn Touhami, S. Radi and Z. Rais, *J. Appl. Electrochem.*, 40 (2010) 1575.
48. A. Samide and B. Tutunaru, *J. Environ. Sci. Health A Tox. Hazard. Subst. Environ. Eng.* 46 (2011) 1713.
49. A. Samide and B. Tutunaru, *Chem. Biochem. Eng. Q.*, 25 (2011) 299.
50. A. Samide, B. Tutunaru, C. Ionescu, P. Rotaru and L. Simoiu, *J. Therm. Anal. Calorim.*, 118 (2014) 631.
51. A.S. Fouda, H.A. Mostafa and H.M. El-Abbasy, *J. Appl. Electrochem.*, 40 (2010) 163.
52. M.I. Awad, *J. Appl. Electrochem.*, 36 (2006) 1163.
53. B. Zerga, B. Hammouti, M. Ebn Touhami, R. Tourir, M. Taleb, M. Sfaira, M. Bennajeh and I. Forssal, *Int. J. Electrochem. Sci.*, 7 (2012) 471.
54. A. Samide, B. Tutunaru, Catalin Negrila and I. Prunaru, *Spectrosc. Lett.*, 45 (2012) 55.
55. A. Samide, P. Rotaru, C. Ionescu, B. Tutunaru, A. Moanță and V. Barragan-Montero, *J. Therm. Anal. Calorim.*, 118 (2014) 651.